Bioactive clerodane diterpenes of giant goldenrod (*Solidago gigantea* Ait.) root extract

Ágnes M. Móricz [a,*], Dániel Krüzselyi [a], Péter G. Ott [a], Zsófia Garádi [b], Szabolcs Béni [b], Gertrud E. Morlock [c], József Bakonyi [a]

[a] *Plant Protection Institute, Centre for Agricultural Research, Herman O. Str. 15, 1022 Budapest, Hungary*
[b] *Department of Pharmacognosy, Faculty of Pharmacy, Semmelweis University, Üllői Str. 26, 1085 Budapest, Hungary*
[c] *Chair of Food Science, Institute of Nutritional Science, and TransMIT Center of Effect-Directed Analysis, Justus Liebig University Giessen, Heinrich-Buff-Ring 26-32, 35392 Giessen, Germany*

ABSTRACT

Giant goldenrod (*Solidago gigantea* Ait.) root extract was screened for bioactive compounds by high-performance thin-layer chromatography (HPTLC), coupled with effect-directed analysis including antibacterial (*Bacillus subtilis* F1276, *B. subtilis* subsp. *spizizenii*, *Aliivibrio fischeri* and *Xanthomonas euvesicatoria*), antifungal (*Fusarium avenaceum*) and enzyme inhibition (acetyl- and butyrylcholinesterases, α- and β-glucosidases and α-amylase) assays. Compounds of six multipotent zones (Sg1-Sg6) were characterized by HPTLC-heated electrospray ionization-high-resolution mass spectrometry (HRMS) and HPTLC-Direct Analysis in Real Time-HRMS. Apart from zone Sg3, containing three compounds, a single characteristic compound was detectable in each bioactive zone. The bioassay-guided isolation using preparative-scale flash chromatography and high-performance liquid chromatography provided eight compounds that were identified by NMR spectroscopy as clerodane diterpenes. All isolates possessed inhibiting activity against at least one of the tested microorganisms.

© 2020 The Author(s). Published by Elsevier B.V.
This is an open access article under the CC BY license (http://creativecommons.org/licenses/by/4.0/)

1. Introduction

A continuously higher qualitative and quantitative supply of agricultural raw materials can meet the increasing demand of the food and feed industry. To improve plant production, appropriate pest management is needed, using effective agrochemicals that are more and more difficult to find due to the emerging (multi)resistance in pathogens against the generally used agents [1,2]. Therefore, many research projects are aimed at discovering effective agrochemicals with new chemical base structure and possibly with low toxicity and fast biodegradability. In the last decade synthetic approaches have not resulted in new antibacterial agents, and the target-based drug discovery also brought disappointment [3]. Purposeful tracking, characterization and isolation of bioactive compounds from natural sources can be achieved by bioassay-guided processes, comprising extraction, fractionation and purification steps, all associated with biomonitoring [4,5]. The high-throughput, relatively cheap effect-directed analysis (EDA) is

enabled by high-performance thin-layer chromatography (HPTLC) combined with bioactivity assays [4,6,7]. EDA is a useful tool to point to individual bioactive compounds (according to the selected assay) separated from a complex matrix, *e.g.,* plant extract. The characterization of potent compounds can easily be achieved by HPTLC-mass spectrometry (MS) using various ionization interfaces [8].

The genus *Fusarium* contains more than twenty species that are among the most important filamentous fungal pathogens on crops, causing economic losses via significant yield reductions and mycotoxin contaminations by this harmful secondary metabolites [9]. In Europe, *Fusarium avenaceum* is one of the dominant *Fusarium* species, causing diseases including head blight of cereals, root rot of legumes and dry rot of potato [10,11]. The pathogen produces several harmful mycotoxins, such as moniliformin, beauvericin and enniatins [12]. Several *Fusarium* species have been introduced for TLC-bioautography. Among them, TLC-direct bioautography, in which diffusion of bioactive substances through agar layer is eliminated, *F. culmorum* [13], *F. sambucinum* [14], *F. oxysporum* [15,16], *F. lateritium* [17], *F. virguliforme* [17], *F. solani* [15] and *F. proliferatum* [15] have been exploited. As an inoculum, their spore (conidium) suspensions were used for the detection of the ger-

mination and/or mycelial growth inhibition by separated bioactive compounds. The inhibition zone was indicated by the lack of visible fungal hyphae, however, vital dyes [15,16] or iodine vapor [18] significantly improved the detectability. Conidial suspension of *F. avenaceum* has been used for dot blot test [18], which is similar to direct bioautography, but the TLC adsorbent is only used to hold the sample, not to separate its components. Spore germination and hyphal growth are distinct biological processes, thus, to assess inhibition of the fungal growth independently of germination, a hyphal segments (practically, their suspension) are required. The use of mycelial growth inhibitors are useful in plant protection as they prevent local spread of the fungal pathogen. So far, neither an HPTLC adsorbent nor a mycelial suspension have been applied for direct bioautography of *Fusarium* species.

Solidago gigantea (giant goldenrod) is native to North America. About 250 years ago, it was introduced to Europe as an ornamental and has become an exceptionally successful invasive and competitive species in most European countries with an abundant biomass [19]. It is widespread in whole Europe and a serious invader of abandoned fields, forest edges and river banks [20]. Goldenrod is also a medicinal plant and listed in the European Pharmacopoeia as *Solidaginis herba* (the whole or cut dried flowering aerial part of either *S. gigantea* Ait. and/or *S. canadensis* L.) used to treat disorders of the urinary tract, prostate and kidney. The goldenrod extract was shown to display favourable antibacterial [21], antifungal [22], insecticidal [23] and anti-obesity [24] activities that can be attributed to its essential oil [25], phenolics [26], saponins [27] and diterpenes [28].

Recently, *S. gigantea* root extract was reported to have antihyperglycaemic (α- and β-glucosidase and α-amylase inhibitory) and cholinesterase inhibitory effects in a screening of five goldenrod species [29]. The present study targeted the detailed characterization and bioprofiling of the giant goldenrod root extract using HPTLC-EDA. The discovered active compounds against enzymes, bacteria (*Bacillus subtilis, Aliivibrio fischeri* and *Xanthomonas euvesicatoria*) and fungus (*F. avenaceum*) were characterized by HPTLC-heated electrospray ionization (HESI)-high resolution (HR)MS and HPTLC-direct analysis in real time (DART)-HRMS. The bioassay-guided isolated compounds were identified by NMR and their antimicrobial activity was confirmed by HPTLC-antimicrobial tests.

2. Materials and methods

2.1. Materials

HPTLC or TLC silica gel 60 F_{254} plates or foils and MS-grade methanol were supplied by Merck (Darmstadt, Germany). Formic acid, vanillin, potassium hydroxide, calcium carbonate, sodium chloride and analytical grade solvents used for layer and flash chromatography were purchased from Reanal (Budapest, Hungary), Th. Geyer (Renningen, Germany) or Sigma-Aldrich (Steinheim, Germany). Gradient grade methanol, acetonitrile (Molar Chemicals, Budapest, Hungary) and pure water produced by a Millipore Direct-Q3 UV system (Merck) were used for HPLC. Gentamicin, methanol-d_4 (99.8%), acetylcholinesterase lyophilisate (from *Electrophorus electricus*, AChE), butyrylcholinesterase (from horse serum, BChE), Fast Blue Salt B (95%), α-glucosidase solution (from *Saccharomyces cerevisiae*), 2-naphthyl-β-D-glucopyranoside, α-amylase (from pig pancreas) and 2-chloro-p-nitrophenyl-α-D-maltotrioside (CNP-G3) were from Sigma. 2-Naphthyl-α-D-glucopyranoside was from Fluorochem (Karlsruhe, Germany). α-Naphthyl acetate was from Panreac (Barcelona, Spain). β-Glucosidase (from almond) was purchased from Carl Roth (Karlsruhe, Germany). Gram-positive *Bacillus subtilis* subsp. *spizizenii* soil bacterium (DSM 618) was from Merck and *B. subtilis* (strain F1276) from József Farkas, Central Food Research Institute, Bu-

dapest, Hungary. Gram-negative, naturally luminescent marine bacterium *Aliivibrio fischeri* (DSM 7151) were obtained from Leibniz Institute DSMZ, German Collection of Microorganisms and Cell Cultures, Berlin, Germany. The Hungarian paprika pathogen *Xanthomonas euvesicatoria* was obtained by János Szarka, Primordium Kft., Budapest, Hungary. *Fusarium avenaceum* strain IMI 319947 was from CABI-IMI Culture Collection, Egham, UK. 3-[4,5-Dimethylthiazol-2-yl]-2,5-diphenyltetrazoliumbromide (MTT), 2,3,5-triphenyl-tetrazolium chloride (TTC) and 2-(4-iodophenyl)-3-(4-nitrophenyl)-5-phenyl-2H-tetrazolium chloride (INT) were from Carl Roth and Sigma, respectively. Vegetable juice (V8) was bought at the local market. Tryptone was from Microtrade (Budapest, Hungary), yeast extract form Scharlau (Barcelona, Spain) and benomyl (Fundazol 50WP) from Chinoin ZRT. (Budapest, Hungary).

2.2. Sample preparation

Roots of *Solidago gigantea* Ait. were collected in February 2017 (young shoots), August 2017 (full flowering) and July 2019 (full flowering) in the Great Plain, Hungary (N 46° 41′ 52.1" E 19° 03′ 3.6" Alt. 90 m). The fresh root was gently washed with water, chopped, dried at room temperature and ground (Bosch MKM6000, Stuttgart, Germany). Powdered samples were macerated in ethanol (150 mg/mL) for 24 h. The filtered crude extract (17 mg dry weight/mL) was used for HPTLC and isolation. Isolated compounds were dissolved in ethanol (2.5 mg/mL).

2.3. HPTLC method

Root extracts (1–2 μL/band for antimicrobial tests and 5 μL/band for enzyme tests) and isolated compounds (0.2–0.5 μL/band for antimicrobial tests and 2 μL/band for reagent) were applied as 6-mm bands with 8-10 mm track distance onto the HPTLC plate (Automated TLC Sampler ATS4 or ATS3, CAMAG, Muttenz, Switzerland) at 8 mm distance from the bottom. HPTLC separation was carried out with *n*-hexane – isopropyl acetate – acetone 16:3:1, *V/V/V* (MP1) [29] or *n*-hexane – isopropyl acetate – acetic acid 40:9:1, *V/V/V* (MP2) up to a migration distance of 70 mm (Twin Trough Chamber TTC, CAMAG). Plates were dried in a cold stream of air (5 min). Residues of acetic acid were eliminated by a 20-min drying (Automatic Developing Chamber ADC2, CAMAG) or by potassium hydroxide in the opposite TTC trough for 2 h [30]. The excess of potassium hydroxide was evaporated by a stream of cold air for 15 min. The plate was cut (blade or smartCUT Plate Cutter, CAMAG) into segments for various bioactivity assays or derivatization with vanillin sulphuric acid reagent (40 mg vanillin, 10 mL ethanol and 200 μL concentrated sulphuric acid, heated at 110 °C for 5 min and documented at UV 365 nm and white light illumination in transmittance mode). The chromatograms were detected by a UV lamp and digital camera (Cybershot DSC-HX60, Sony, Neu-Isenburg, Germany) or TLC Visualizer Documentation System or TLC Scanner 4 (both CAMAG).

2.4. HPTLC-EDA

Bacterial cell suspensions were prepared and the antibacterial effect was detected, as described in previous methods using *B. subtilis* F1276 [31], *B. subtilis* subsp. *spizizenii* [32], *A. fischeri* [33,34] and *X. euvesicatoria* [31]. Briefly, the developed, neutralized plates were immersed into the cell suspensions for 6 s. The dark antibacterial zones in the bioautograms of luminescent *A. fischeri* were instantly documented (BioLuminizer, CAMAG or iBright™ FL1000 Imaging System, Thermo Fisher Scientific, Budapest, Hungary). In the cases of non-luminescent bacteria, bioautograms were visualized after a 2-h incubation (100% humidity at appropriate temperature) by staining with an aqueous MTT solution (1 mg/mL) fol-

lowed by a 0.5-h incubation. Colorless (bright) antibacterial zones were obtained against a bluish background.

The reported HPTLC-AChE/BChE [35], HPTLC-α/β-glucosidase and HPTLC-α-amylase [29] inhibition assays were applied. For the α-amylase assay, the plate was immersed into the substrate solution (1.4 mg/mL CNP-G3 in ethanol), dried for 2 min in a stream of cold air, immersed in the buffered α-amylase enzyme solution, incubated at 37 °C for 15 min and dried. For the other enzyme assays, each plate was dipped into the respective buffered enzyme solution and incubated for 15-20 min at 37 °C. The AChE/BChE and α/β-glucosidase autograms were immersed in a solution of the substrate (α-naphthyl acetate and 2-naphthyl-α/β-D-glucopyranoside, respectively, followed by a 10-min incubation) and the chromogenic reagent (Fast Blue Salt B) and dried. Documentation was performed at white light illumination in the reflectance mode. Colorless (bright) zones indicated the active compounds against a yellow (α-amylase) or violet (AChE/BChE and α/β-glucosidase) background. The detailed enzyme inhibition assay methods are presented in the supplementary data.

The *F. avenaceum* strain was grown on V8 agar medium (80 mL water, 20 mL Campbell's V8 vegetable juice, 100 μL 1 M potassium hydroxide to adjust to pH 6.5, 0.4 m/m% calcium carbonate, 1.8 g agar) at 20 °C in the dark. Lysogenic broth (LB, 20 mL; 10 g/L tryptone, 5 g/L yeast extract and 10 g/L sodium chloride) was inoculated in a 100 mL Erlenmeyer flask with the fungal culture grown on the V8 agar plate and shaken at 120 rpm at 21 °C for 3 days in the dark. The mycelium was washed with LB to eliminate the conidia and cut to small pieces with a sterile rotor-stator type homogenizer (Model TR-10, Tekmar, Cincinnati, OH) for 2 min two times. The mycelium suspension was diluted to OD_{600} 0.4 - 0.8. Developed HPTLC plates were dipped into the mycelium suspension for 6 s and incubated in a vapor chamber at 21 °C for 48 - 72 h. The lack of visible white fungal hyphae indicated the inhibition zones. By spraying aqueous INT solution (1 mg/mL; cca 2 mL/plate) on the bioautograms followed by a 1-h incubation, the contrast was enhanced by revealing bright inhibition zones against a violet background. An aqueous solution of benomyl (1 µL/band; 25 mg/mL, active ingredient of Fundazol 50WP) was applied as positive control (at the edge of the developed plate before immersion in the mycelium suspension).

To evaluate the effects on *B. subtilis* subsp. *spizizenii* and AChE, the (bio)autograms were scanned in the fluorescence mode at 546 and 533 nm using the mercury and wolfram lamp (TLC Scanner 4, CAMAG). Images were processed with ImageJ software (NIH, Bethesda, MA, USA).

2.5. HPTLC-HRMS and HRMS-MS

Prewashed plates (with methanol−water 4:1, *V/V* dried at 100 °C for 20 min) were used and separated zones of interest were marked. For HPTLC-HESI-HRMS, the quaternary pump (Ultimate LPG-3400 XRS, Dionex Softron, Germering, Germany) guided the methanol at a flow rate of 0.1 mL/min through the oval elution head (4 mm x 2 mm) of the PlateExpress interface (Advion, Ithaca, NY, USA) to the HESI-II installed at the hybrid quadrupole-orbitrap mass spectrometer (Q Exactive Plus, Thermo Fisher Scientific, Bremen, Germany). Spray voltage was 3.5 kV, capillary temperature was 270 °C, and nitrogen as sheath and auxiliary gas (20 and 10 arbitrary units, respectively) was produced by an SF2 compressor (Atlas Copco Kompressoren und Drucklufttechnik, Essen, Germany). Full scan HRMS spectra were recorded in the negative and positive ionization mode in the range of *m/z* 50 - 750 with a resolution of 280,000, automatic gain control target of 3×10^6 and maximum injection time of 100 ms. Isolated compounds and flash chromatographic fractions were directly injected by flow injection analysis (FIA) in the mentioned HRMS system (spray voltage 3.5 kV, capil-

lary temperature 270 °C, sheath and auxiliary gases at 20 and 10 arbitrary units, respectively). Tandem mass spectra were acquired as parallel reaction monitoring with mass isolation of the target molecule (fragmentation/collision energy of 40 - 60 eV, resolution of 17,500, automatic gain control target of 2×10^5, maximum injection time of 100 ms and isolation window of *m/z* 2 for *m/z* 50). Operation and data processing were performed with Xcalibur 3.0.63 software (Thermo).

A DART interface (IonSense, Saugus, MA, USA) modified for scanning of HPTLC plates [36] was coupled to the mentioned HRMS system. The ion source was operated with an initial needle voltage of 4 kV and grid voltage of 50 V in the positive ionization mode using helium (99.999%) at a flow rate of 3.0 L min^{-1} and temperature of 500 °C. Spectra were recorded in the full scan (*m/z* 100 − 750) at a resolution of 280,000, automatic gain control target of 5×10^4 and maximum injection time of 50 ms. The DART scanning speed was 0.2 mm s^{-1}. The extracted ion current (EIC) chromatograms were processed with a Gauss smoothing function width of 11 points.

2.6. Preparative column chromatography

The extract (10 mL, dried and re-suspended in *n*-hexane) was fractionated with Combiflash NextGen 300 (Teledyne Isco, Lincoln, NE, USA) flash chromatography system. Separation was performed on a RediSep Rf Gold silica gel column (20-40 µm, 12 g; Teledyne Isco) at a flow rate of 30 mL/min with a gradient of *n*-hexane (A) and acetone (B): 0-0.5 min, 0% B; 0.5-8.5 min 0-30% B. The chromatogram was monitored by absorbance measurement at 215 nm. Compounds in the collected active fractions were further fractionated and purified. HPLC separations (conditions are in Table 1) were carried out using an LC–MS-2020 system (Shimadzu, Kyoto, Japan), including binary gradient solvent pump, vacuum degasser, thermostated autosampler, column oven, photodiode detector and electrospray ionization (ESI)-MS system. Instrument control and data acquisition were performed with the LabSolutions 5.42v program (Shimadzu). First, analytical methods were developed that were scaled up using a semi-preparative column. The analytical separation of the fractions (5 µL) on a Gemini C18 column (250 mm x 4.6 mm ID, 5 µm particle size, Phenomenex, Torrance, CA, USA) at 35 °C with a step-wise gradient was detected by MS (nitrogen as nebulizer gas, flow rate 1.5 L/min, drying gas (nitrogen) flow rate 15 L/min, interface temperature 350 °C, heatblock temperature 400 °C, desolvation line temperature 250 °C and detector voltage 4.5 kV). Full scan mass spectra were recorded in the positive and negative ionization mode in the range of *m/z* 150 − 900 with a scan speed of 5000 amu/s. The semi-preparative separation of the fractions (100 µL) on a Gemini C18 column (250 mm x 10 mm ID, 10 µm particle size, Phenomenex) was detected in the UV. Compound Sg6 (90 µL) was purified on a Kinetex pentafluorophenyl (PFP) column (100 mm x 4.6 mm ID, 2.6 µm particle size, Phenomenex) at 35 °C. The fractionation/purification was repeated up to 10-times. The combined fractions were investigated by HPTLC-assays, dried with a rotary evaporator (Rotavapor R-134, Büchi, Flawil, Switzerland) at 40 °C and transferred to NMR spectroscopy.

2.7. NMR

NMR spectra were recorded in deuterated methanol (Methanol-d_4, 99.8 atom % D, containing 0.05% tetramethylsilane) on a Bruker Avance III HD 600 (600/150 MHz) instrument equipped with a Prodigy cryo-probehead at 295 K. The pulse programs were taken from the Bruker software library (TopSpin 3.5). Chemical shifts (δ) and coupling constants (*J*) are given in ppm and in Hz, respectively. ^{1}H chemical shifts are given in ppm relative to tetramethyl-

Table 1
Detailed description of preparative and analytical scale HPLC methods

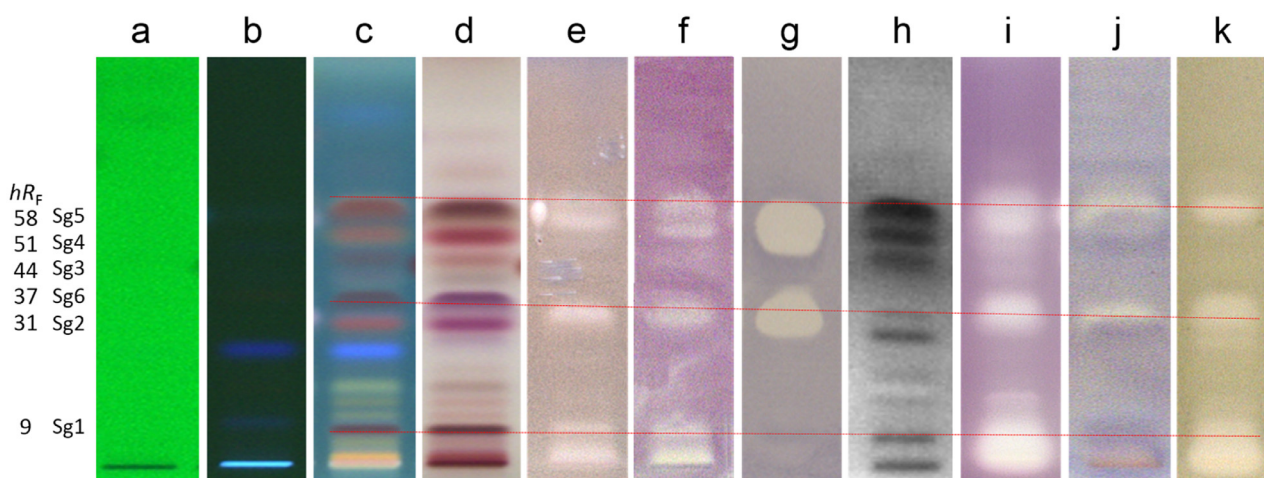| Method	Extract	Column	Eluent A	Eluent B	Gradient	Flow rate (mL/min) 0.8; 3.5 enter 0.7; 3.5 enter 0.7; 4 enter 0.8	Collected peaks
1	flash fractions	Gemini C18, 250 mm x 10 mm, 10 µm *Gemini C18, 250 mm x 4.6 mm, 5 µm*	5% aqueous methanol	acetonitrile	0-14 min 75% B 14-20 min 100% B 20-26 min 75% B	4 *0.8*	Sg1, Sg2, Sg3a+Sg3b, Sg4+Sg3c, Sg5
2	Sg3a + Sg3b		5% aqueous methanol	methanol	0-18 min 75% B 18-21 min 100% B 21-25 min 75% B	3.5*0.7*	Sg3a, Sg3b
3	Sg4 + Sg3c		5% aqueous methanol	methanol	0-18 min 80-88% B 18-21 min 100% B 21-25 min 80% B	3.5 *0.7*	Sg4, Sg3c
4	Sg5		5% aqueous methanol	acetonitrile + 0.1% formic acid	0-14 min 75% B 14-20 min 100% B 20-26 min 75% B	4*0.8*	Sg5
5	flash fraction 13	Kinetex PFP, 100 mm x 4.6 mm, 2.6 µm	5% aqueous methanol	methanol	0-12.5 min 65-77% B 12.5-15.5 min 100% B 15.5-19.5 min 65% B	0.6	Sg6

Fig. 1. HPTLC chromatograms and autograms of the *S. gigantea* root extract, developed with *n*-hexane – isopropyl acetate – acetone 16:3:1 (*V/V/V*, MP1) and detected at UV 254 nm (a), UV 365 nm (b), after derivatization with vanillin sulphuric acid reagent at UV 365 nm (c) and white light illumination (d; also e-g and i-k) AChE (e), BChE (f), *B. subtilis* subsp. *spizizenii* (g), *A. fischeri* (h, greyscale image of the bioluminescence), α-glucosidase (i), β-glucosidase (j) and α-amylase (k).

silane (δ=0.00 ppm). ^{13}C chemical shifts are given in ppm relative to the NMR solvent (δ=49.00 ppm). The complete ^{1}H and ^{13}C assignments were deduced using conventional 1D (^{1}H NMR, ^{13}C NMR, DeptQ) and 2D (^{1}H-^{1}H COSY, ^{1}H-^{13}C edHSQC ^{1}H-^{13}C HMBC and ^{1}H-^{1}H NOESY) measurements.

3. Results and discussion

3.1. HPTLC-EDA

Two methods were investigated for the separation of the giant goldenrod root compounds (Figs. 1 and 2) on HPTLC plates silica gel 60 with either *n*-hexane – isopropyl acetate – acetone 16:3:1 *V/V/V* (MP1, [29]) or *n*-hexane – isopropyl acetate – acetic acid 40:9:1 *V/V/V* (MP2). Both separations detected at white light illumination after derivatization with the universal vanillin sulphuric acid reagent, provided the six distinguishable colored zones Sg1-Sg6 that were hardly detectable without the derivatization (Figs. 1a, 1b, 2a and 2b). MP2 resulted in higher hR_F values, which was obvious for Sg5 and Sg6, indicating a potential acidic character. MP2 chromatograms required a neutralization step before EDA. Compounds with antidiabetic (anti-hyperglycaemic) effect could be used for the treatment of type 2 diabetes and obesity that are the most common and increasing chronic diseases in the world. In the HPTLC-EDA screening with MP1 (Fig. 1e-k), the zones Sg5 (at hR_F

58) and Sg6 (at hR_F 37) showed α-glucosidase, β-glucosidase and α-amylase inhibition. The application zone up to hR_F 9 was also effective in α-glucosidase and α-amylase assays. Cholinesterase inhibitors are of therapeutic interest in the Alzheimer disease, the most common cause of dementia and one of the major public health issues. Compounds in the zones Sg1 (hR_F 9), Sg4 (hR_F 51), Sg5 and Sg6 inhibited AChE and BChE (Fig. 1e and f). However, with MP2 and neutralization, BChE inhibitory zones of Sg1 (hR_F 17) and Sg4 (hR_F 55) were lacking (Fig. 2f). Multipotent compounds are generally not favorable for pharmaceutical use, however, these compounds can become lead compounds toward the development of more specific, thus more useful derivatives.

Antibacterial agents are widely required for the fight against infectious plant, animal and human diseases caused by pathogenic bacterial and fungal strains. In the antibacterial assays, the Gram-positive *B. subtilis* subsp. *spizizenii* soil bacterium, the Gram-negative, naturally luminescent marine *A. fischeri* and the Gram-negative paprika pathogen *X. euvesicatoria* were employed. In the *B. subtilis* assay, Sg1 and compounds at an even lower hR_F were only active in the MP2 separation (Figs. 1g and 2g). All marked zones were active against *A. fischeri* (Figs. 1h and 2h) and *X. euvesicatoria* (Fig. 2i), except for Sg3 at the given amount applied. Additionally, Sg6 showed activity against *A. fischeri* only on acid-free bioautograms. The positions of the bioactive zones were con-
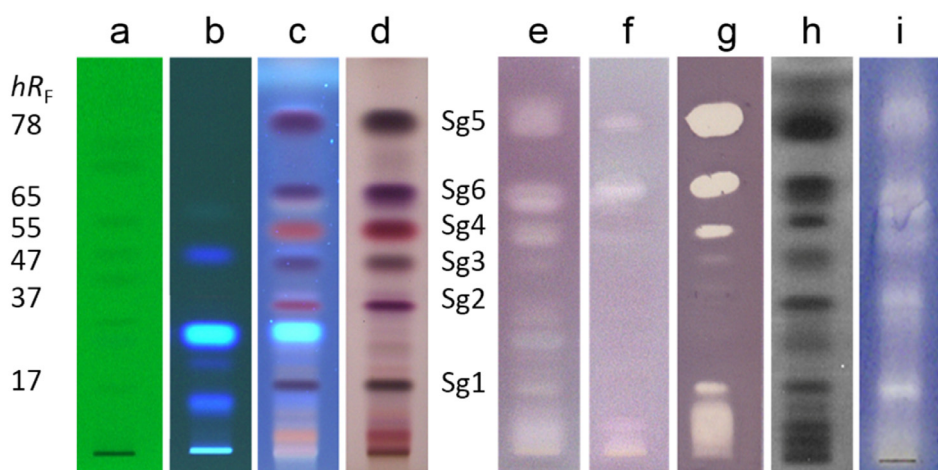
Fig. 2. HPTLC chromatograms and autograms of the *S. gigantea* root extract, developed with *n*-hexane – isopropyl acetate – acetic acid 40:9:1 (*V/V/V*, MP2) and detected at UV 254 nm (a), UV 365 nm (b), after derivatization with vanillin sulphuric acid reagent at UV 365 nm (c) and white light illumination (d; also e-g and i), AChE (e), BChE (f), *B. subtilis* subsp. *spizizenii* (g), *A. fischeri* (h, greyscale image of the bioluminescence) and *X. euvesicatoria* (i) assays.
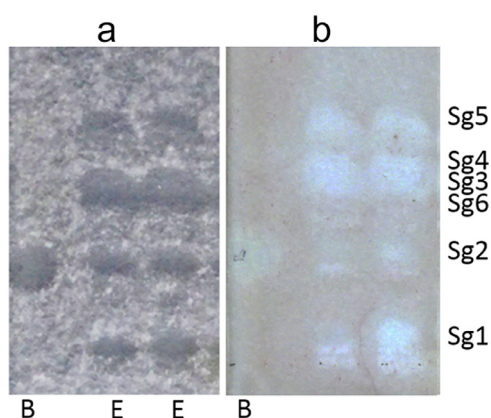

Fig. 3. HPTLC-*F. avenaceum* bioautogram of giant goldenrod root extract (E, 2 and 3 μL/band) and positive control benomyl (B, 25 μg/band) developed with *n*-hexane – isopropyl acetate – acetone 16:3:1 (*V/V/V*, MP1) and detected at white light illumination after the bioassay (a) and subsequent staining with INT (b).

firmed by densitometry or videodensitometry of the MP2 bioautograms (Fig. S1). The results of the enzyme assays are in agreement with our previous observations [29], however, the influence of an acidic development and its neutralization on the outcome needs further study.

An HPTLC-antifungal assay using plant pathogenic fungus *F. avenaceum* was newly developed. *F. avenaceum* grew well on V8 solid agar medium and the surface of a 5 cm petri dish was totally occupied by its white hyphae within 2-3 days after inoculation by an agar block (5 mm x 5 mm) in the center. Similarly, a dense mycelium suspension was obtained within 3 days by shaking the liquid inoculum (LB medium) at 21 °C. After cutting the mycelium to small fragments, the suspension was initially diluted to reach an OD_{600} of 0.4. Dipping a plate into this suspension, an appropriate mycelium growth was optically reached after a 3-days incubation in a vapor chamber at 21 °C (Fig. 3), indicating as mycelium growth inhibition the antifungal activity of zones Sg1, Sg2, Sg3, Sg4 and Sg5. For detection, the three different tetrazolium dyes INT, MTT and TTC were investigated, whereby the fastest coloration was achieved with INT, which colored the hyphae violet (Figs. 3 and S2). Compared to the 3-days-old mycelium suspension, the 1-day-old inoculum did not grow as fast on the HPTLC plate, and the

5-days-old was found to be less sensitive (Fig. S3). In agreement to our previous study, no characteristic inhibition was observed using older microbial (bacterial) cells in the stationary and death phases [37]. The staining procedure enabled the reduction of the incubation time to 2 days. The incubation time could not be shortened - by increasing the OD_{600} of the mycelial inoculum from 0.2 to 0.8 - whithout a loss in discernability of the inhibition zones. In the final protocol, the mycelium suspension at an OD_{600} of 0.4 was incubated for 2 days on the HPTLC plate and then detected by INT staining, followed by a 1-h incubation and documentation under white light illumination in the reflectance mode (Fig. S4).

3.2. HPTLC-MS

The bioactive compound zones Sg1-Sg6 were separated with MP1 and characterized by HPTLC-HESI-HRMS and HPTLC-DART-HRMS (Table 2, Fig. S5). HPTLC-HESI$^+$-HRMS signals were obtained for all six compound zones, but the signal intensities were very low for Sg1 at *m/z* 341.2088 [M+Na]$^+$ ($C_{20}H_{30}O_3Na^+$) and Sg2 at *m/z* 355.1879 [M+Na]$^+$ ($C_{20}H_{28}O_4Na^+$). However, it still allowed the assignment of their molecular formulae. The recorded mass signals for the Sg3 zone at *m/z* 337.1776 [M+Na]$^+$ ($C_{20}H_{26}O_3Na^+$) and at very low intensity *m/z* 325.2140 [M+Na]$^+$ ($C_{20}H_{30}O_2Na^+$) indicated the coelution of at least two compounds. As discussed later, even three compounds Sg3a-c were identified in this zone. An intense mass signal was recorded at *m/z* 339.1931 [M+Na]$^+$ ($C_{20}H_{28}O_3Na^+$) for Sg4. For Sg5 and Sg6, prominent mass signals were obtained in both ionization mode at *m/z* 339.1931 [M+Na]$^+$ ($C_{20}H_{28}O_3Na^+$) and *m/z* 437.2304 [M+Na]$^+$ ($C_{25}H_{34}O_5Na^+$) as well as at *m/z* 315.1956 [M-H]$^-$ and *m/z* 413.2304 [M-H]$^-$, respectively. These zone assignments were successfully confirmed by separation with MP2 and HPTLC-ESI-MS (Fig. S6). In the positive and negative ionization mode, also the sodium-methanol-adducts [M+CH$_3$OH+Na]$^+$ and sodium-acetate-adducts of the respective compounds were observed, which was caused by a too low drying gas flow.

With exception of Sg1, all other compound zones gave mass signals by HPTLC-DART-HRMS (Table 2, Figs. 4 and S7). In the positive ionization mode, the protonated molecule [M+H]$^+$ was detected for Sg3 and Sg5. Further, ammonium adducts [M+NH$_4$]$^+$ and dehydroxylated molecular ions [M-OH]$^+$ were prominent. In the negative ionization mode, the deprotonated molecules were
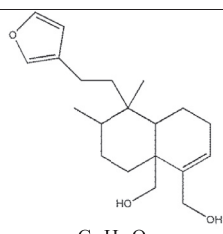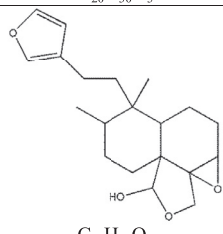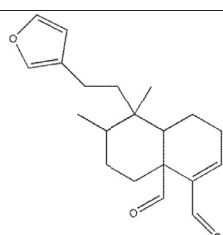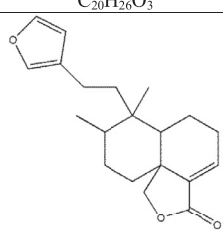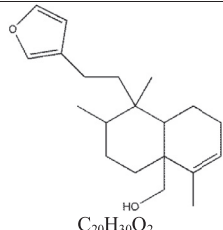
detected for the Sg5 and Sg6 zones, and also the dimer for Sg5 and a $C_5H_7O_2^-$ fragment for Sg6.

3.3. Isolation of the active compounds

The root extract (10 mL) was fractionated by flash chromatography on a silica gel column, resulting in nineteen fractions (fr1-fr19), which were studied by HPTLC-Vis after derivatization with the vanillin sulphuric acid reagent (Fig. S8a and b). The six fractions containing the previously characterized bioactive compounds (fr10-fr14 and fr17) were subjected to RP-HPLC-DAD-ESI-MS anal-
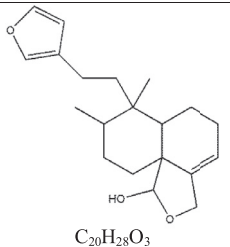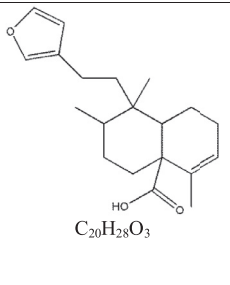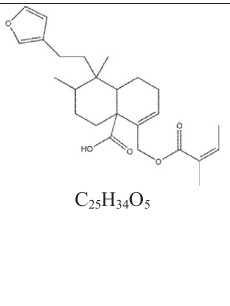
ysis (Fig. S8c, Table 2). The HPLC method 1 (Table 1) was found to be suitable for compound isolation in the Sg1, Sg2 and Sg5 zones, whereby the latter zone was tailing. Acid-free mobile phases were selected to avoid acid-analyte reactions, which might impair the bioactivity result. However, in the case of Sg5, the collected peak was further purified with an acidic conditioning in the HPLC method 4. The Sg6 compound zone was eluted from the C18 column during the washing step. Thus, its retention was achieved on a PFP column (HPLC method 5). The HPTLC separation revealed two co-eluting compounds in each of the HPLC peaks at 10-min (Sg3a and Sg3b) and 12.5-min retention times (Sg3c and Sg4) (Fig.

Table 2
Chemical structures, molecular formulae and assignments (using orthogonal techniques) of the eight discovered bioactive compounds in *S. gigantea* root extract.

Compound	Chemical structure and molecular formula	HPTLC-HESI-HRMS m/z	FIA-HESI-HRMS/MS m/z	HPTLC-DART-HRMS m/z	HPLC-ESI-MS m/z
Sg1	$C_{20}H_{30}O_3$	+341.20878 [M+Na]$^+$; $C_{20}H_{30}O_3Na^+$ (at low intensity) error: 0.2 ppm	not fragmentable	not detectable	+341 [M+Na]$^+$ +659 [2M+Na]$^+$
Sg2	$C_{20}H_{28}O_4$	+355.18787 [M+Na]$^+$; $C_{20}H_{28}O_4Na^+$ (at low intensity) error: 0.3 ppm	(-331.1916) 287.2009 $C_{19}H_{27}O_2^-$ 219.1747 $C_{15}H_{23}O^-$ 189.1279 $C_{13}H_{17}O^-$	+348.21707 [M+NH$_4$]$^+$; $C_{20}H_{30}O_4N^+$ +332.22229 [M-OH+NH$_3$]$^+$; $C_{20}H_{30}O_3N^+$ +315.19578 [M-OH]$^+$; $C_{20}H_{27}O_3^+$ +297.18522 [M-OH-H$_2$O]$^+$; $C_{20}H_{25}O_2^+$ +273.18513 [M-C$_2$OH-H$_2$O]$^+$; $C_{18}H_{25}O_2^+$	+297 [M-OH-H$_2$O]$^+$ +315 [M-OH]$^+$ +333 [M+H]$^+$ +355 [M+Na]$^+$ -331 [M-H]$^-$
Sg3a	$C_{20}H_{26}O_3$	+337.17764 [M+Na]$^+$; $C_{20}H_{26}O_3Na^+$ error: 0.6 ppm	(+315.19548) 297.1844 $C_{20}H_{25}O_2^+$ 279.1741 $C_{20}H_{23}O^+$ 269.1891 $C_{19}H_{25}O^+$ 251.1790 $C_{19}H_{23}^+$ 215.1427 $C_{15}H_{19}O^+$	+332.22235 [M+NH$_4$]$^+$; $C_{20}H_{30}O_3N^+$ +315.19585 [M+H]$^+$; $C_{20}H_{27}O_3^+$ +297.18526 [M-OH]$^+$; $C_{20}H_{25}O_2^+$	+297 [M-OH]$^+$ +315 [M+H]$^+$ +337 [M+Na]$^+$ +369 [M+CH$_3$OH+Na]$^+$ +651 [2M+Na]$^+$
Sg3b	$C_{20}H_{26}O_3$	+337.17764 [M+Na]$^+$; $C_{20}H_{26}O_3Na^+$ error: 0.6 ppm	(+315.19548) 297.1844 $C_{20}H_{25}O_2^+$ 279.1742 $C_{20}H_{23}O^+$ 269.1897 $C_{19}H_{25}O^+$ 251.1790 $C_{19}H_{23}^+$ 233.1533 $C_{15}H_{21}O_2^+$ 215.1428 $C_{15}H_{19}O^+$ 189.1275 $C_{13}H_{17}O^+$ 125.0599 $C_7H_9O_2^+$	+332.22235 [M+NH$_4$]$^+$; $C_{20}H_{30}O_3N^+$ +315.19586 [M+H]$^+$; $C_{20}H_{27}O_3^+$ +297.18526 [M-OH]$^+$; $C_{20}H_{25}O_2^+$ +273.18521 [M-C$_2$OH]$^+$; $C_{18}H_{25}O_2^+$	+315 [M+H]$^+$ +337 [M+Na]$^+$ +369 [M+CH$_3$OH+Na]$^+$ +651 [2M+Na]$^+$
Sg3c	$C_{20}H_{30}O_2$	+325.21400 [M+Na]$^+$; $C_{20}H_{30}O_2Na^+$ (at very low intensity) error: 0.6 ppm	(-301.2169) 273.2213 $C_{19}H_{29}O^-$ 257.2276 $C_{19}H_{29}^-$ 229.1953 $C_{17}H_{25}^-$ 191.1432 $C_{13}H_{19}O^-$ 171.1382 $C_{10}H_{19}O_2^-$ 87.0085 $C_4H_7O_2^-$ 71.0493 $C_4H_7O^-$	not identified	+325 [M+Na]$^+$

(continued on next page)

Table 2 (*continued*)

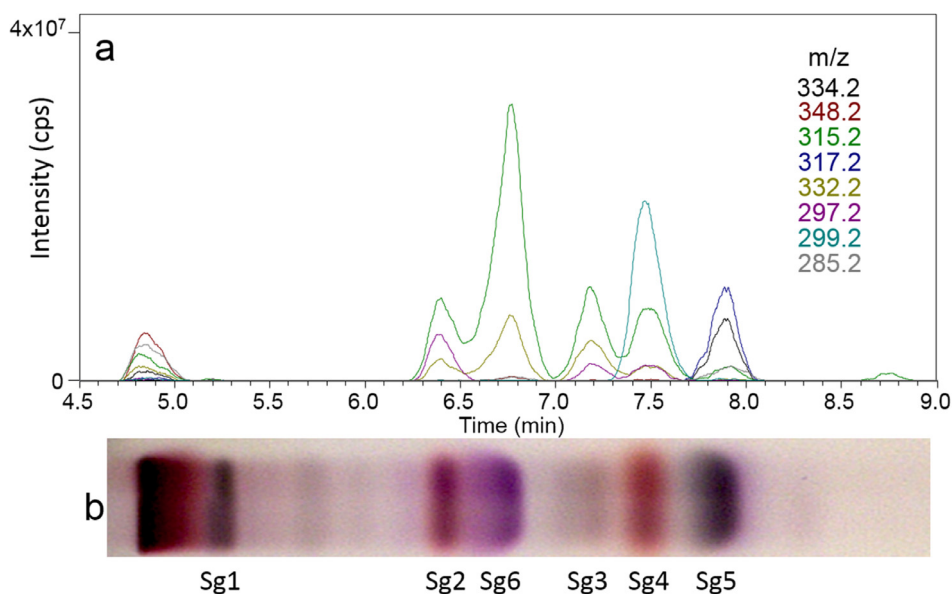|					
Sg4	$C_{20}H_{28}O_3$	+339.19312 [M+Na]$^+$; $C_{20}H_{28}O_3Na^+$ error: 0.2 ppm	not fragmentable	+332.22223 [M+NH$_4$]$^+$; $C_{20}H_{30}O_3N^+$ +315.19583 [M-OH+O]$^+$; $C_{20}H_{27}O_3^+$ +299.20081 [M-OH]$^+$; $C_{20}H_{27}O_2^+$ +275.20084 [M-C$_2$OH]$^+$; $C_{18}H_{27}O_2^+$	+299 [M-OH]$^+$ +339 [M+Na]$^+$ +371 [M+CH$_3$OH+Na]$^+$ +655 [2M+Na]$^+$
Sg5	$C_{20}H_{28}O_3$	+339.19307 [M+Na]$^+$; $C_{20}H_{28}O_3Na^+$ error: 0.1 ppm -315.19565 [M-H]$^-$; $C_{20}H_{27}O_3^-$ error: 0.5 ppm	(-315.1967) -271.2062 $C_{19}H_{27}O^-$	+334.23788 [M+NH$_4$]$^+$; $C_{20}H_{32}O_3N^+$ +317.21140 [M+H]$^+$; $C_{20}H_{29}O_3^+$ +287.20084 [M-CO-H]$^+$; $C_{19}H_{27}O_2^+$ -315.19669 [M-H]$^-$; $C_{20}H_{27}O_3^-$ -631.40100 [2M-H]$^-$; $C_{40}H_{55}O_6$	-315 [M-H]$^-$ +339 [M+Na]$^+$ -653 [M-2H+Na]$^-$
Sg6	$C_{25}H_{34}O_5$	+437.23042 [M+Na]$^+$; $C_{25}H_{34}O_5Na^+$ error: 1.3 ppm -413.23041 [M-H]$^-$; $C_{25}H_{33}O_5^-$ error: 1.4 ppm	(-413.2304) -99.0448 $C_5H_7O_2^-$ (+437.2293) +337.1759 $C_{20}H_{26}O_3Na^+$ +293.1865 $C_{19}H_{26}ONa^+$ +123.0411 $C_5H_8O_2Na^+$ +81.0338 $C_5H_5O^+$	+332.22237 [M-C$_5$H$_7$O$_2$+NH$_3$]$^+$; $C_{20}H_{30}O_3N^+$ +315.19585 [M-C$_5$H$_7$O$_2$]$^+$; $C_{20}H_{27}O_3^+$ -413.23346 [M-H]$^-$; $C_{25}H_{33}O_5^-$	+299 +315 +437 [M+Na]$^+$ +851 [2M+Na]$^+$ +873 [2M+CH$_3$OH+Na]$^+$ +895 [2M+2CH$_3$OH+Na]$^+$ -413 [M-H]$^-$ -827 [2M-H]$^-$ -849 [2M+CH$_3$OH-H]$^-$

Fig. 4. EIC chromatograms of scanning HPTLC-DART-MS in the positive ionization mode (a) and respective HPTLC chromatogram of the bioactive giant goldenrod root components separated with *n*-hexane – isopropyl acetate – acetone 16:3:1 (*V/V/V*, MP1) detected at white light illumination after derivatization with vanillin sulphuric acid reagent (b).
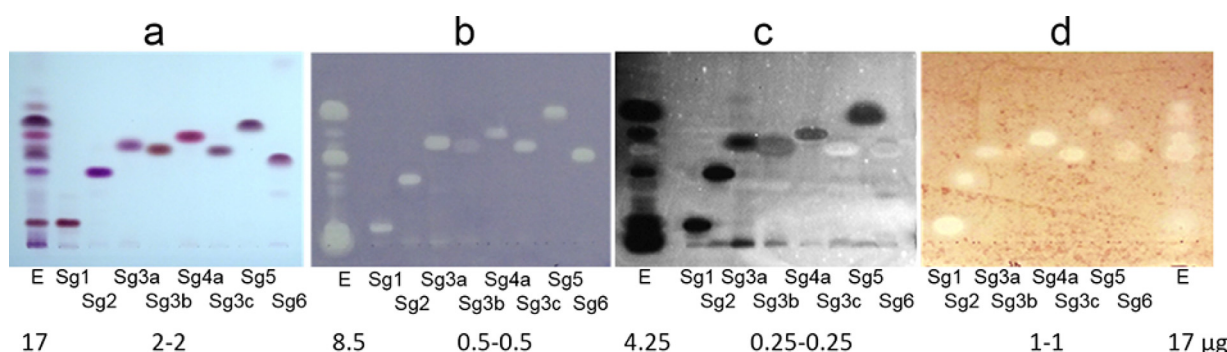
Fig. 5. Confirmation of purity and bioactivity: HPTLC chromatogram and autograms of the bioactive compounds Sg1-Sg6 isolated from giant goldenrod root extract (E) separated with *n*-hexane – isopropyl acetate – acetone 16:3:1 (*V/V/V*, MP1) and detected at white light illumination (a, b and d) after derivatization with the vanillin–sulphuric acid reagent (a), *B. subtilis* F1276 (b), *A. fischeri* (c, greyscale image of the bioluminescence) and *F. avenaceum* (d) assays.

S8c). For their separation, HPLC methods 2 and 3 were developed, respectively. Eight compounds were isolated using a preparative C18 column (Fig. S9) and an analytical PFP column (Fig. S10). These were assigned as Sg1 (1.1 mg), Sg2 (1.6 mg), Sg3a (0.9 mg), Sg3b (1.0 mg), Sg3c (1.5 mg), Sg4 (2.1 mg), Sg5 (2.2 mg) and Sg6 (6.2 mg) according to their respective HPTLC zones.

3.4. Identification and characterization of the isolated compounds

The isolates were analyzed by FIA-HESI-HRMS/MS to successfully confirm that their identity was not changed during the isolation procedure, including fractionation and purification. Fragmentation of the respective sodium adduct of the compounds was not observed except for Sg6 (Table 2), and thus, also the respectively less intense protonated or deprotonated molecules were selected. The intense deprotonated molecules of Sg5 and Sg6 were easily fragmented.

The HPTLC-Vis analysis of the isolates (separated with MP1, Fig. 5a, and MP2, Fig. S11 and detected after derivatization with the vanillin sulphuric acid reagent) showed that only a single compound was present in all previously assigned zones, except for three compounds (Sg3a-c) detected in Sg3. All isolates were active against *B. subtilis*, whereby Sg3b had only a weak activity (Fig. 5b). Most isolated compounds strongly affected *A. fischeri*, whereby Sg3b showed a mild effect, and Sg3c and Sg6 no response at all (Fig. 5c). All compounds except Sg3b suppressed the growth of *F. avenaceum* mycelium with varying degrees of effectiveness (Fig. 5d). Although for the Sg3 and Sg6 zones of the root extract, no activity against *B. subtilis* and *F. avenaceum*, respectively, was evident, their respective isolates did have an antimicrobial effect. This was explained by the fact that their concentrations in the root extract were too low to reach the minimum inhibitory concentration. The eight isolated compounds were most probably responsible for the enzyme inhibiting activity, but this was not confirmed. The purity of the eight isolates was adequate, as confirmed by NMR analysis (Table S1, Figs. S12-S59). The eight compounds were identified as the furan-containing clerodane diterpenoids: a glycol (Sg1, known also as kingidiol, white solid), an epoxy-hemiacetal (Sg2, oil), a dialdehyde (Sg3a, white solid), the clerodane lactone (Sg3b, oil, also known as hautriwaic lactone), an alcohol (Sg3c, oil), a hemiacetal (Sg4, oil), the solidagoic acid A (Sg5, white solid) and the solidagoic acid B (Sg6, white solid), which have been described as components of *S. gigantea* roots [38-40] (Table 2). NMR data in literature supported the identification of the isolated compounds [28,38,39,41,42]. Antimicrobial [43-46], cytotoxic [45-47] and anti-inflammatory effect [48] of several clerodane diterpenes isolated from plants have been described. Among *Solidago* species, clerodane diterpenes of European goldenrod (*S. virgaurea*) were pub-

lished to inhibit *Staphylococcus aureus* [42]. The activity of three of our isolated compounds has already been studied mainly against insects. Sg5 was inactive, Sg1 caused the retardation of follicle development in mosquito ovaries [28] and displayed moderate toxicity against brine shrimp (*Artemia salina*) [49]. In contrast to Sg1, Sg3b was found as anti-feedant and repellent agent in a study of mealworms (*Tenebrio molitor*) [50]. Antiplasmodial (antimalarial) and antileishmanial (inhibition of the intracellular parasite *Leishmania donovani*) effects of Sg3b were also observed, whereby it did not show cytotoxicity against Vero cells (African green monkey kidney fibroblast) [51]. Except for the new antifungal profiling, the HPTLC-bioprofiling of the root extract has been previously reported by us, however, it lacked in identification of the active compounds by HRMS and NMR. To the best of our knowledge, this is the first report about the antimicrobial profile of the eight isolated *S. gigantea* root diterpenoids. Further investigations are intended to evaluate their possible use as safe and effective pesticides, especially fungicides.

Conclusions

The newly developed HPTLC-*F. avenaceum* assay was demonstrated for the first time using mycelium suspension. It allowed a cost-effective screening of complex plant extracts for antifungal (mycelium growth inhibiting) compounds in *S. gigantea* root extract. Further bioprofiling of the extract against various bacterial strains and enzymes by HPTLC-EDA pointed to multi-potent compounds. The comparison of the use of a neutral *versus* acidic mobile phase demonstrated that the latter can influence the bioassay result. The state of the art combination of HPTLC-bioactivity assays, HPTLC-HESI-HRMS, HPTLC-DART-HRMS, preparative-scale column chromatography (flash chromatography and HPLC) and NMR provided eight multi-potent clerodane diterpenoids in goldenrod. It is the first report on the antifungal, antibacterial and enzyme inhibiting activity of the multipotent isolates, which showed potential as lead compounds especially for various infectious plant diseases.

Declaration of Competing Interest

The authors declare that they have no known competing financial interests or personal relationships that could have appeared to influence the work reported in this paper.

Acknowledgment

Supplementary materials

Supplementary material associated with this article can be found, in the online version, at doi:10.1016/j.chroma.2020.461727.

References

[1] B.A. Lorsbach, T.C. Sparks, Innovations in agrochemical discovery and the role of metabolism, bioavailability and formulations, Pest Manag. Sci. 73 (2017) 655–657, doi:10.1002/ps.4533.

[2] M. Hahn, The rising threat of fungicide resistance in plant pathogenic fungi: *Botrytis* as a case study, J. Chem. Biol. 7 (2014) 133–141, doi:10.1007/s12154-014-0113-1.

[3] P.S. Hoffman, Antibacterial Discovery: 21st Century Challenges, Antibiotics 9 (2020) 213, doi:10.3390/antibiotics9050213.

[4] Á.M. Móricz, P.G. Ott, T.T. Häbe, A. Darcsi, A. Böszörményi, Á. Alberti, D. Krüzselyi, P. Csontos, S. Béni, G.E. Morlock, Effect-directed discovery of bioactive compounds followed by highly targeted characterization, isolation and identification, exemplarily shown for *Solidago virgaurea*, Anal. Chem. 88 (2016) 8202–8209, doi:10.1021/acs.analchem.6b02007.

[5] W. Jonker, M.H. Lamoree, C.J. Houtman, J. Kool, Methodologies for effect-directed analysis: environmental applications, food analysis, and drug discovery, in: Anal. Biomol. Interact. by Mass Spectrom, Wiley-VCH Verlag GmbH & Co. KGaA, Weinheim, Germany, 2015, pp. 109–163, doi:10.1002/9783527673391.ch4.

[6] G. Morlock, W. Schwack, Hyphenations in planar chromatography, J. Chromatogr. A 1217 (2010) 6600–6609, doi:10.1016/j.chroma.2010.04.058.

[7] G.E. Morlock, Chromatography combined with bioassays and other hyphenations – the direct link to the compound indicating the effect, in: 2014: pp. 101–121. 10.1021/bk-2014-1185.ch005.

[8] G. Morlock, W. Schwack, Coupling of planar chromatography to mass spectrometry, TrAC Trends Anal. Chem. 29 (2010) 1157–1171, doi:10.1016/j.trac.2010.07.010.

[9] J. Yu, R.H. Proctor, D.W. Brown, K. Abe, K. Gomi, M. Machida, F. Hasegawa, W.C. Nierman, D. Bhatnagar, T.E. Cleveland, Genomics of economically significant *Aspergillus* and *Fusarium* species, in: 2004: pp. 249–283. 10.1016/S1874-5334(04)80013-3.

[10] S. Vogelgsang, M. Sulyok, A. Hecker, E. Jenny, R. Krska, R. Schuhmacher, H.-R. Forrer, Toxigenicity and pathogenicity of *Fusarium poae* and *Fusarium avenaceum* on wheat, Eur. J. Plant Pathol. 122 (2008) 265–276, doi:10.1007/s10658-008-9279-0.

[11] A.T. Pollard, P.A. Okubara, Real-time PCR quantification of *Fusarium avenaceum* in soil and seeds, J. Microbiol. Methods 157 (2019) 21–30, doi:10.1016/j.mimet.2018.12.009.

[12] S. Uhlig, A.C. Gutleb, U. Thrane, A. Flåøyen, Identification of cytotoxic principles from *Fusarium avenaceum* using bioassay-guided fractionation, Toxicon 46 (2005) 150–159, doi:10.1016/j.toxicon.2005.03.005.

[13] A.L. Homans, A. Fuchs, Direct bioautography on thin-layer chromatograms as a method for detecting fungitoxic substances, J. Chromatogr. A 51 (1970) 327–329, doi:10.1016/S0021-9673(01)96877-3.

[14] K.D. Burkhead, D.A. Schisler, P.J. Slininger, Pyrrolnitrin Production by biological control agent *Pseudomonas cepacia* B37w in culture and in colonized wounds of potatoes, Appl. Environ. Microbiol. 60 (1994) 2031–2039, doi:10.1128/AEM.60.6.2031-2039.1994.

[15] N. Kasanah, L.L. Farr, A. Gholipour, D.E. Wedge, M.T. Hamann, Metabolism and resistance of *Fusarium* spp. to the manzamine alkaloids via a putative retro Pictet-Spengler reaction and utility of the rational design of antimalarial and antifungal agents, Mar. Biotechnol. 16 (2014) 412–422, doi:10.1007/s10126-014-9557-0.

[16] R.E. Beale, D. Pitt, The antifungal properties of *Minimedusa polyspora*, Mycol. Res. 99 (1995) 337–342, doi:10.1016/S0953-7562(09)80910-6.

[17] G.L. Gallardo, N.I. Peña, G.M. Cabrera, Neric acid derivatives produced by the honey bee fungal entomopathogen *Ascosphaera apis*, Phytochem. Lett. 1 (2008) 155–158, doi:10.1016/j.phytol.2008.07.008.

[18] F. Hadacek, H. Greger, Testing of antifungal natural products: methodologies, comparability of results and assay choice, Phytochem. Anal. 11 (2000) 137–147, doi:10.1002/(SICI)1099-1565(200005/06)11:3⟨137:AID-PCA514⟩3.0.CO;2-I.

[19] M. Szymura, T.H. Szymura, Interactions between alien goldenrods (*Solidago* and *Euthamia* species) and comparison with native species in Central Europe, Flora - Morphol. Distrib. Funct. Ecol. Plants. 218 (2016) 51–61, doi:10.1016/j.flora.2015.11.009.

[20] G. Jakobs, E. Weber, P.J. Edwards, Introduced plants of the invasive *Solidago gigantea* (Asteraceae) are larger and grow denser than conspecifics in the native range, Divers. Distrib. 10 (2004) 11–19, doi:10.1111/j.1472-4642.2004.00052.x.

[21] Barbara Kołodziej, Antibacterial and antimutagenic activity of extracts aboveground parts of three *Solidago* species: *Solidago virgaurea* L., *Solidago canadensis* L. and *Solidago gigantea* Ait, J. Med. Plants Res. 5 (2011), doi:10.5897/JMPR11.1098.

[22] D. Webster, P. Taschereau, R.J. Belland, C. Sand, R.P. Rennie, Antifungal activity of medicinal plant extracts; preliminary screening studies, J. Ethnopharmacol 115 (2008) 140–146, doi:10.1016/j.jep.2007.09.014.

[23] G. Benelli, R. Pavela, K. Cianfaglione, D.U. Nagy, A. Canale, F. Maggi, Evaluation of two invasive plant invaders in Europe (*Solidago canadensis* and *Solidago gigantea*) as possible sources of botanical insecticides, J. Pest Sci. 92 (2019) 805–821 (2004), doi:10.1007/s10340-018-1034-5.

[24] Z. Wang, J.H. Kim, Y.S. Jang, C.H. Kim, J.-Y. Lee, S.S. Lim, Anti-obesity effect of *Solidago virgaurea* var. *gigantea* extract through regulation of adipogenesis and lipogenesis pathways in high-fat diet-induced obese mice (C57BL/6N), Food Nutr. Res. 61 (2017) 1273479, doi:10.1080/16546628.2016.1273479.

[25] D. Kalemba, B. Thiem, Constituents of the essential oils of four micropropagated *Solidago* species, Flavour Fragr. J. 19 (2004) 40–43, doi:10.1002/ffj.1271.

[26] J. Radusiene, M. Marska, L. Ivanauskas, V. Jakstas, B. Karpaviciene, Assessment of phenolic compound accumulation in two widespread goldenrods, Ind. Crops Prod. 63 (2015) 158–166, doi:10.1016/j.indcrop.2014.10.015.

[27] G. Reznicek, M. Freiler, M. Schader, U. Schmidt, Determination of the content and the composition of the main saponins from *Solidago gigantea* Ait. using high-performance liquid chromatography, J. Chromatogr. A 755 (1996) 133–137, doi:10.1016/S0021-9673(96)00571-7.

[28] S.-H. Lee, H.-W. Oh, Y. Fang, S.-B. An, D.-S. Park, H.-H. Song, S.-R. Oh, S.-Y. Kim, S. Kim, N. Kim, A.S. Raikhel, Y.H. Je, S.W. Shin, Identification of plant compounds that disrupt the insect juvenile hormone receptor complex, Proc. Natl. Acad. Sci. 112 (2015) 1733–1738, doi:10.1073/pnas.1424386112.

[29] Á.M. Móricz, M. Jamshidi-Aidji, D. Krüzselyi, A. Darcsi, A. Böszörményi, P. Csontos, S. Béni, P.G. Ott, G.E. Morlock, Distinction and valorization of 30 root extracts of five goldenrod (*Solidago*) species, J. Chromatogr. A 1611 (2020) 460602, doi:10.1016/j.chroma.2019.460602.

[30] Á.M. Móricz, P.G. Ott, I. Yüce, A. Darcsi, S. Béni, G.E. Morlock, Effect-directed analysis via hyphenated high-performance thin-layer chromatography for bioanalytical profiling of sunflower leaves, J. Chromatogr. A 1533 (2018) 213–220, doi:10.1016/j.chroma.2017.12.034.

[31] Á.M. Móricz, T.T. Häbe, A. Böszörményi, P.G. Ott, G.E. Morlock, Tracking and identification of antibacterial components in the essential oil of *Tanacetum vulgare* L. by the combination of high-performance thin-layer chromatography with direct bioautography and mass spectrometry, J. Chromatogr. A 1422 (2015) 310–317, doi:10.1016/j.chroma.2015.10.010.

[32] M. Jamshidi-Aidji, G.E. Morlock, Bioprofiling of unknown antibiotics in herbal extracts: Development of a streamlined direct bioautography using *Bacillus subtilis* linked to mass spectrometry, J. Chromatogr. A 1420 (2015) 110–118, doi:10.1016/j.chroma.2015.09.061.

[33] S. Krüger, O. Urmann, G.E. Morlock, Development of a planar chromatographic method for quantitation of anthocyanes in pomace, feed, juice and wine, J. Chromatogr. A 1289 (2013) 105–118, doi:10.1016/j.chroma.2013.03.005.

[34] Á.M. Móricz, T.T. Häbe, P.G. Ott, G.E. Morlock, Comparison of high-performance thin-layer with overpressured layer chromatography combined with direct bioautography and direct analysis in real time mass spectrometry for tansy root, J. Chromatogr. A 1603 (2019) 355–360, doi:10.1016/j.chroma.2019.03.068.

[35] S. Hage, G.E. Morlock, Bioprofiling of Salicaceae bud extracts through high-performance thin-layer chromatography hyphenated to biochemical, microbiological and chemical detections, J. Chromatogr. A 1490 (2017) 201–211, doi:10.1016/j.chroma.2017.02.019.

[36] T.T. Häbe, G.E. Morlock, Improved desorption/ionization and ion transmission in surface scanning by direct analysis in real time mass spectrometry, Rapid Commun. Mass Spectrom. 30 (2016) 321–332, doi:10.1002/rcm.7434.

[37] Á. Móricz, N. Adányi, E. Horváth, P. Ott, E. Tyihák, Applicability of the BioArena system to investigation of the mechanisms of biological effects, J. Planar Chromatogr. – Mod. TLC 21 (2008) 417–422, doi:10.1556/JPC.21.2008.6.4.

[38] M.S. Henderson, R. McCrindle, D. McMaster, Constituents of *Solidago* species. Part V. Non-acidic diterpenoids from *Solidago gigantea* var. *serotina*, Can. J. Chem. 51 (1973) 1346–1358, doi:10.1139/v73-201.

[39] T. Anthonsen, M.S. Henderson, A. Martin, R.D.H. Murray, R. McCrindle, D. McMaster, Constituents of *Solidago* species. Part IV. Solidagoic acids A and B, diterpenoids from *Solidago gigantea* var. *serotina*, Can. J. Chem. 51 (1973) 1332–1345, doi:10.1139/v73-200.

[40] T. Anthonsen, M.S. Henderson, A. Martin, R. McCrindle, R.D.H. Murray, Furan-containing diterpenoids from *Solidago serotina* Ait, Acta Chem. Scand. 22 (1968) 351–352, doi:10.3891/acta.chem.scand.22-0351.

[41] T.G. Payne, P.R. Jefferies, The chemistry of *Dodonaea* spp - IV, Tetrahedron 29 (1973) 2575–2583, doi:10.1016/0040-4020(73)80176-0.

[42] C.M. Starks, R.B. Williams, M.G. Goering, M. O'Neil-Johnson, V.L. Norman, J.-F. Hu, E. Garo, G.W. Hough, S.M. Rice, G.R. Eldridge, Antibacterial clerodane diterpenes from goldenrod (*Solidago virgaurea*), Phytochemistry 71 (2010) 104–109, doi:10.1016/j.phytochem.2009.09.032.

[43] V.K. Gupta, N. Tiwari, P. Gupta, S. Verma, A. Pal, S.K. Srivastava, M.P. Darokar, A clerodane diterpene from *Polyalthia longifolia* as a modifying agent of the resistance of methicillin resistant *Staphylococcus aureus*, Phytomedicine 23 (2016) 654–661, doi:10.1016/j.phymed.2016.03.001.

[44] A. Bisio, A.M. Schito, S.N. Ebrahimi, M. Hamburger, G. Mele, G. Piatti, G. Romussi, F. Dal Piaz, N. De Tommasi, Antibacterial compounds from *Salvia adenophora* Fernald (*Lamiaceae*), Phytochemistry 110 (2015) 120–132, doi:10.1016/j.phytochem.2014.10.033.

[45] P. Chawengrum, J. Boonsombat, P. Kittakoop, C. Mahidol, S. Ruchirawat, S. Thongnest, Cytotoxic and antimicrobial labdane and clerodane diterpenoids from *Kaempferia elegans* and *Kaempferia pulchra*, Phytochem. Lett. 24 (2018) 140–144, doi:10.1016/j.phytol.2018.02.009.

[46] A.L. Pfeifer Barbosa, A. Wenzel-Storjohann, J.D. Barbosa, C. Zidorn, C. Peifer, D. Tasdemir, S.S. Çiçek, Antimicrobial and cytotoxic effects of the *Copaifera reticulata* oleoresin and its main diterpene acids, J. Ethnopharmacol. 233 (2019) 94–100, doi:10.1016/j.jep.2018.11.029.

[47] P.M.P. Ferreira, G.C.G. Militão, D.J.B. Lima, N.D. de, J. Costa, K.da C. Machado, A.G. dos Santos, A.J. Cavalheiro, V.da S. Bolzani, D.H.S. Silva, C. Pessoa, Morphological and biochemical alterations activated by antitumor clerodane diterpenes, Chem. Biol. Interact. 222 (2014) 112–125, doi:10.1016/j.cbi.2014.10.015.

[48] Y. Wang, J. Lin, Q. Wang, K. Shang, D.-B. Pu, R.-H. Zhang, X.-L. Li, X.-C. Dai, X.-J. Zhang, W.-L. Xiao, Clerodane diterpenoids with potential anti-inflammatory activity from the leaves and twigs of *Callicarpa cathayana*, Chin. J. Nat. Med. 17 (2019) 953–962, doi:10.1016/S1875-5364(19)30118-9.

[49] C. Labbe, M. Castillo, M. Hernandez, Diterpenoids from *Baccharis lejía*, Phytochemistry 30 (1991) 1607–1611, doi:10.1016/0031-9422(91)84217-G.

[50] M.E. Sosa, C.E. Tonn, O.S. Giordano, Insect antifeedant activity of clerodane diterpenoids, J. Nat. Prod. 57 (1994) 1262–1265, doi:10.1021/np50111a012.

[51] A.A.da S. Filho, D.O. Resende, M.J. Fukui, F.F. Santos, P.M. Pauletti, W.R. Cunha, M.L.A. Silva, L.E. Gregório, J.K. Bastos, N.P.D. Nanayakkara, In vitro antileishmanial, antiplasmodial and cytotoxic activities of phenolics and triterpenoids from *Baccharis dracunculifolia* D. C. (*Asteraceae*), Fitoterapia 80 (2009) 478–482, doi:10.1016/j.fitote.2009.06.007.